NEAR INERTIAL OSCILLATIONS AT THE SHELF OFF NORTHERN PATAGONIA

ANDRÉS L. RIVAS[1] AND ALBERTO R. PIOLA[2]

(1) Centro Nacional Patagónico (CENPAT-CONICET), Boulevard Brown s/n, (9120) Puerto Madryn, Chubut, Argentina.
(2) Departamento Oceanografía, Servicio de Hidrografía Naval and Departamento de Ciencias de la Atmósfera y los Océanos, Facultad de Ciencias Exactas y Naturales, Universidad de Buenos Aires, Avda. Montes de Oca 2124, (1271) Buenos Aires, Argentina.
E-mail: andres@cenpat.edu.ar, fax: 054 2965 451543.

RESUMO

Quatro séries temporais de correntes obtidas próximas a 43°S sobre a plataforma continental da Patagônia, coletadas entre Setembro/1991 e Agosto/1992, foram filtradas com frequências de corte de 0.049 e 0.068 ciclos por hora (cph) para extrair a componente quase inercial. As séries temporais filtradas têm somente uma pequena atenuação de amplitude quando comparadas aos dados originais e a fase não foi alterada. Em dois fundeios costeiros, onde a coluna d'água é fracamente estratificada a energia contida na banda inercial é desprezível. Sobre plataforma externa o pico inercial é largo, e velocidades máximas são > 25 cm s^{-1}. O vetor velocidade horizontal é quase polarizado circularmente (excentricidade de 1.04) e gira em sentido anti-horário com uma freqüência um pouco maior que a freqüência inercial local. A direção de propagação é para 105° relativos ao norte verdadeiro, aproximadamente perpendicular à costa. A correlação complexa entre correntes filtradas nas profundidades de 17 e 67 m tem uma magnitude de 0.83 e uma diferença de fase de 176°, indicando que o fluxo é dominado pelo primeiro modo baroclínico. A taxa entre as amplitudes acima e abaixo da picnoclina é controlada pela profundidade da picnoclina, como previsto por um modelo de duas camadas. O modelo simples de Pollard & Millard (1970), forçado com o vento de Puerto Madryn**,** reproduziu muitos dos fatores observados das correntes inerciais na camada superficial. A ausência de oscilações inerciais sobre plataforma externa durante o inverno, e a reduzida amplitude costeira durante o período de amostragem, são associadas portanto à reduzida estratificação da coluna de água.

ABSTRACT

Four current time series collected near 43°S on the continental shelf off Patagonia from September 1991 to August 1992 have been band pass filtered with cutoff frequencies of 0.049 and 0.068 cycles per hour (cph) to extract the near-inertial component. The filtered time series have only small amplitude attenuation when compared to the original data and phase is not changed. At two near-shore moorings, where the water column is poorly stratified the energy contained in the inertial band is negligible. At mid-shelf the spectral peak of the inertial band is large and maximum speeds are > 25 cm s^{-1}. The horizontal velocity vector is nearly circularly polarized (eccentricity of 1.04) and rotates counterclockwise with a frequency a few percent greater than the local inertial frequency. The propagation direction is to 105°T, approximately perpendicular to the coast. The complex correlation between filtered currents at 17 and 67 m depth has a magnitude of 0.83 and a phase difference of 176°, indicating that the flow is dominated by the first baroclinic mode. The ratio between observed amplitudes above and below the pycnocline is controlled by pycnocline depth, as predicted by a two-layer model. The simple model of Pollard and Millard (1970) forced with wind data from Puerto Madryn reproduced many of the observed features of the inertial currents in the surface layer. The lack of inertial oscillations in the mid-shelf during Austral winter and the reduced amplitude near the coast throughout the sampling period, are associated to the reduced stratification of the water column.

1 – INTRODUCTION

Oscillations with nearly inertial frequency are a commonly observed oceanic phenomenon. Generally, an "inertial peak" dominates the spectrum of horizontal currents and contributes significantly to the total kinetic energy. The main characteristics of these currents have been widely documented (e.g. Kundu, 1976b and Pollard, 1980). Inertial oscillations generally occur at intervals which last only a few cycles and are correlated with variations in the wind stress. Many observational and theoretical studies suggest that the near-inertial motions can be generated by sudden changes of the surface wind stress (Pollard, 1970; Kundu & Thomson, 1985). At latitudes where the local inertial frequency is close to principal tidal frequencies, inertial motions also can be initiated when tidal energy is transferred into low-frequency baroclinic gravity waves by the interaction of tides and bottom topography (Hendershott, 1973), but this is not the case at 43°S of latitude, where the inertial frequency is about 17.5 hours. The velocity vector is circularly polarized and rotates in a counterclockwise sense (Southern Hemisphere) with a frequency rate slightly higher than the local inertial frequency. Coherence scales for upper-layer motions vary from tens of meters in the vertical to tens of kilometers in the horizontal and horizontal coherence decreases with depth. The phase propagates upwards with the velocity vector rotating in a counterclockwise sense as depth increases (Southern Hemisphere) and kinetic energy propagates towards the seabed, consistent with a mechanism of surface generation. In the coastal region, the amplitude of near-inertial oscillations must decrease toward the coast to match the boundary condition of no flow across the coastline and the spatial structure can be modified due to the bottom topography (Chen et al., 1996).

In 1991, we deployed an array of current meters in the Argentine continental shelf near 43°S. The study area

and mooring locations are shown in Figure 1. The analysis of Rivas (1997) shows that in the moorings closer to the coast, the semi-diurnal band accounts for more than 90% of the total fluctuating kinetic energy; whereas little kinetic energy is found in the inertial and the low-frequency bands. In contrast, the data collected in a mid-shelf mooring show that the inertial band is as energetic as the diurnal and semi-diurnal bands, whereas the low-frequency fluctuations account for almost 20% of the kinetic energy. Glorioso & Flather (1995) carried out a numerical simulation of the tidal flux on the shelf, and the results are in good agreement with the observations of Rivas (1997). Glorioso & Flather (1995) suggested that the increase in the semi-diurnal component towards the coast is associated to a resonance process, and that the intensity of the diurnal component is modulated by topographically trapped components (continental shelf waves) of the diurnal tide. The spatial distribution of low-frequency energy lead Rivas (1997) to associate the low-frequency flow to the interaction between the Malvinas Current and the shelf topography.

These observations show that the inertial oscillations constitute an important part of the kinetic energy measured in the mid-shelf, where they exceed the semi-diurnal component in the near-surface data. Therefore, inertial oscillations can be important in inducing vertical mixing and shear causing the re-suspension of bottom sediments and nutrient redistribution thus having biological implications. The goal of the present work is to analyze these oscillations and to interpret their spatial and temporal variations, including the seasonal scale.
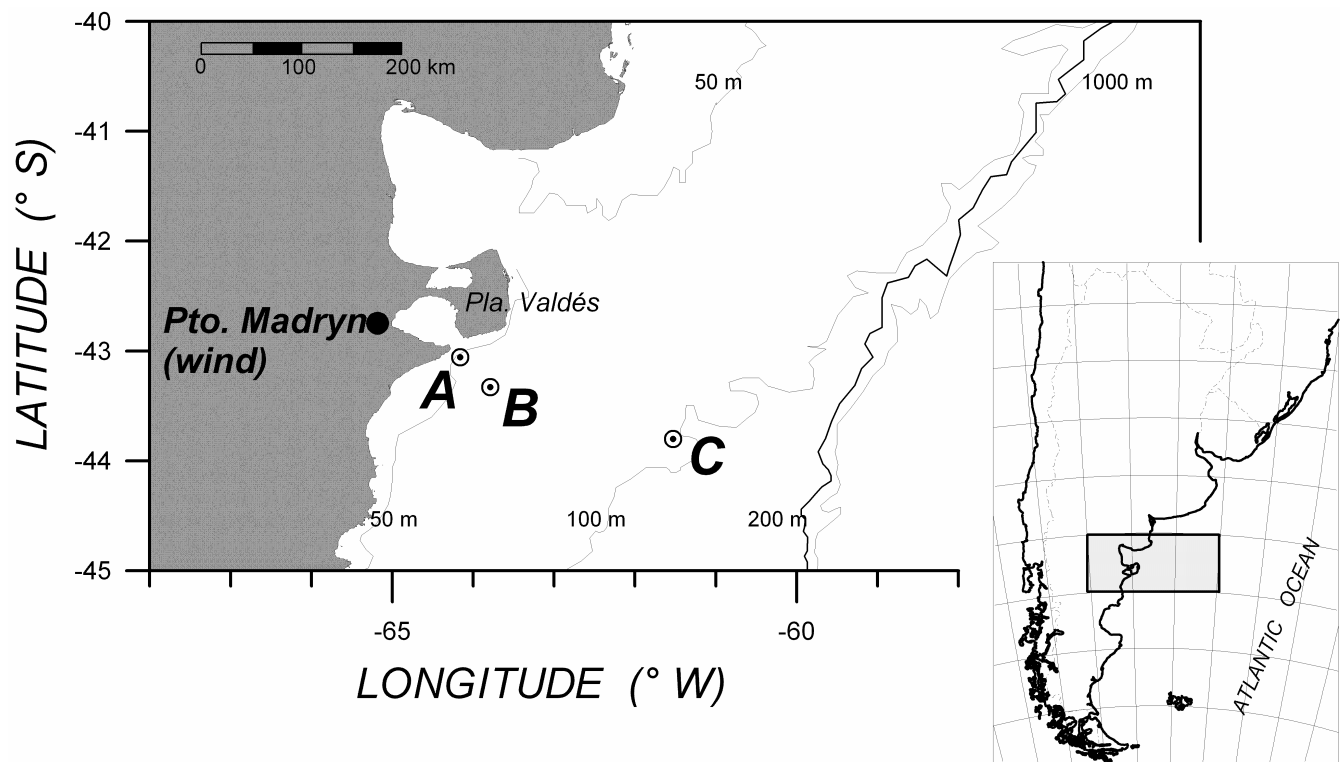

FIGURE 1 – Location of moorings and wind station with bathymetric contours (in meters).

2 – DATA AND METHODS

The current data (summarized in Table 1), the wind records (obtained in Puerto Madryn, 42° 16' S - 65° 02' W) and the hydrographic data (collected during three hydrographic surveys carried out between September 1991 and August 1992) are presented in Charo et al. (1993), Balestrini et al. (1996) and Rivas (1997). The moorings are located along a line running towards the ESE, approximately perpendicular to the coast and the isobaths (Figure 1). In the mooring closer to shore, referred to as site A, current data were obtained at 53 m. At site B,

located 49 km offshore from A, currents were recorded at 27 m and at site C, 191 km further offshore, currents were recorded at 17 and 67 m depth.

TABLE 1 – Summary of spatial and temporal availability of current-meter data.

Number	Latitude S Longitude W	Instrument depth (m)	Water depth (m)	Instrument type	Sampling interval (min)	Start / stop time (yr-mo-day)	Record length (days)
A	42°58.814' 64°12.109'	53.5	65	Neil Brown ACM-2	15	91-09-20 / 92-02-16	149
B	43°19.189' 63°48.764'	27	81	Neil Brown ACM-2	15	91-09-23 / 92-08-03	315
C17	43°45.342' 61°31.444'	17	97	Aanderaa RCM 5	60	91-09-21 / 92-07-03	286
C67	43°45.342' 61°31.444	67	97	Aanderaa RCM 5	60	91-09-21 / 92-02-16	148

In order to preserve only the inertial frequency band and the phase of the original data we applied a Kaiser symmetric band-pass filter to the eastward and northward velocity components. The one-hour sampling intervals at site C were filtered using a 241 element filter, while the 15 minute sampling interval data at sites A and B were filtered with a 961 element filter. In both cases, the ideal cut-off frequencies are 0.049 and 0.068 cycles per hour (cph). Upon application of the filter, the original, finite length inertial signal is spread over additional cycles and the amplitude of the filtered records is reduced compared to that of the pre-filtered series. Kundu (1976b) and Thomson & Hugget (1981) discussed this effect in detail. The peak smearing effect of a narrow band-pass filter and the ability of the filter in suppressing the tidal components ware tested using a synthetic series. The results showed very good filter performance.

3 – ANALYSIS

3.1 – General Characteristics

Figure 2 shows the filtered eastward components from the four current records. In the mooring nearest the coast (site A), there is virtually no inertial signal (<3 cm s^{-1}), and at B, closer to the surface and further offshore, the inertial signal is weak (<8 cm s^{-1}) and is only observed from mid November to late March. On the other hand, the inertial signal found in the mid-shelf mooring (site C) is well defined, both in the near-surface (C17) and in the deeper (C67) observations. The data collected at 17 meters (C17) shows an intermittent signal of several days duration and maximum amplitudes higher than 25 cm s^{-1}. The amplitude obtained within the mixed layer decreases beginning in late March; however, pulses of considerable amplitude are observed in May. At 67 meters (C67) the amplitude of the inertial oscillations is about 50% of the amplitude observed at 17 m, suggesting a downward energy decrease. In agreement with the above observations, the spectral analysis of the original data (Rivas, 1997) suggested that the most intense inertial oscillations occur far from the coast and that their amplitude decreases as depth increases.
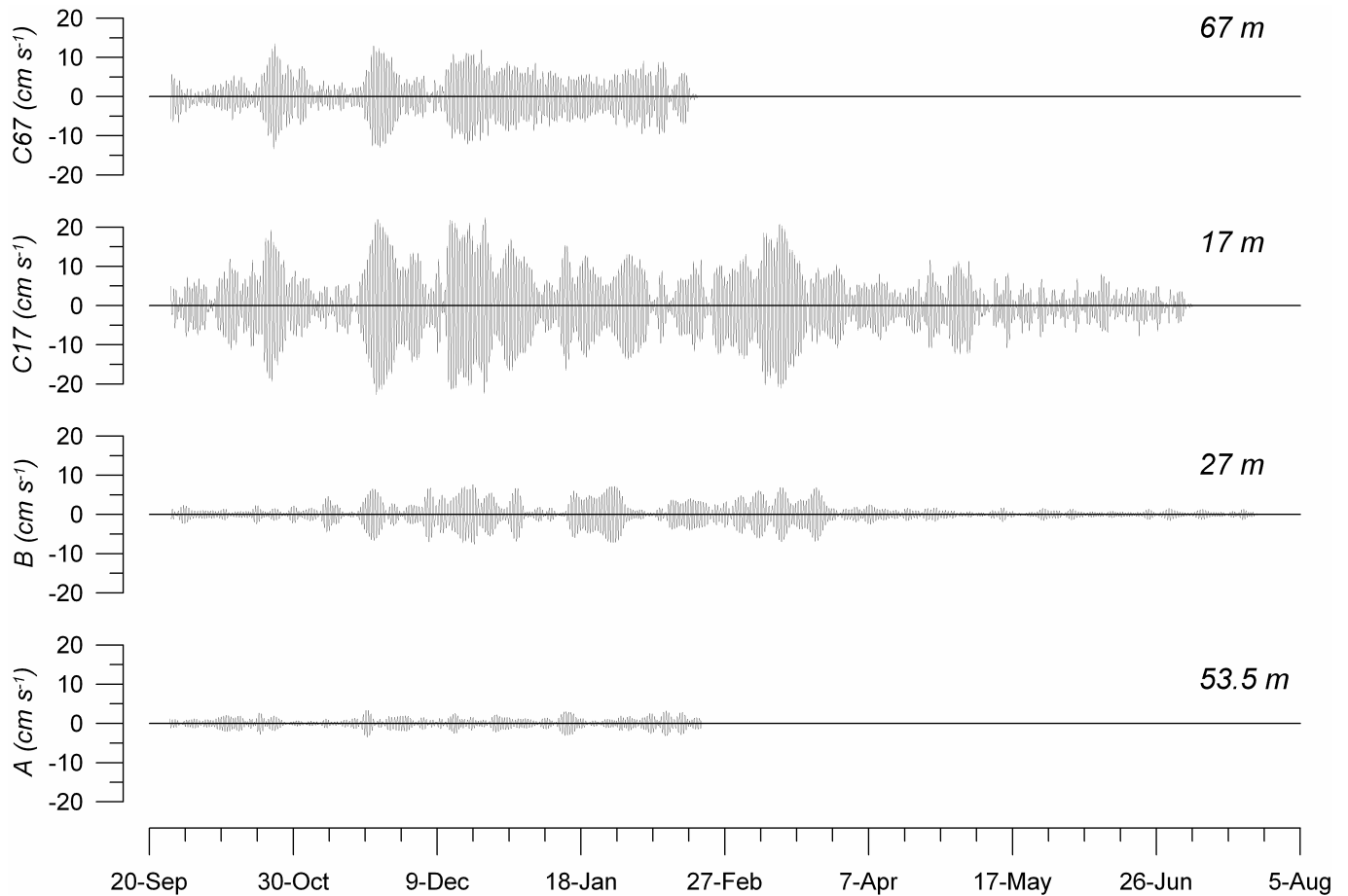
FIGURE 2 – Band-passed eastward velocity component for all instruments.

At all sites the amplitude of the northward velocity component (not shown) is virtually equal to the eastward components. There is a phase difference of approximately 90° between velocity components. A detailed view of both velocity components observed at site C from 20 to 30 October 1991 shows that the horizontal currents are almost circularly polarized in a counterclockwise sense (Figure 3). The mean phase difference between filtered velocity components for each instrument was estimated as

$$d = \cos^{-1} [<u\ v> / (<u^2> <v^2>)^{1/2}]$$

where <> indicates the record length time average. The estimated phase difference at sites A, B, C17 and C67 are 87.7°, 93.8°, 91.2° and 89.8° respectively. The rotary spectra of the filtered series (Figure 4) confirm the counterclockwise rotation, and depict the ability of the filter to preserve the fundamental characteristics of the inertial signal.
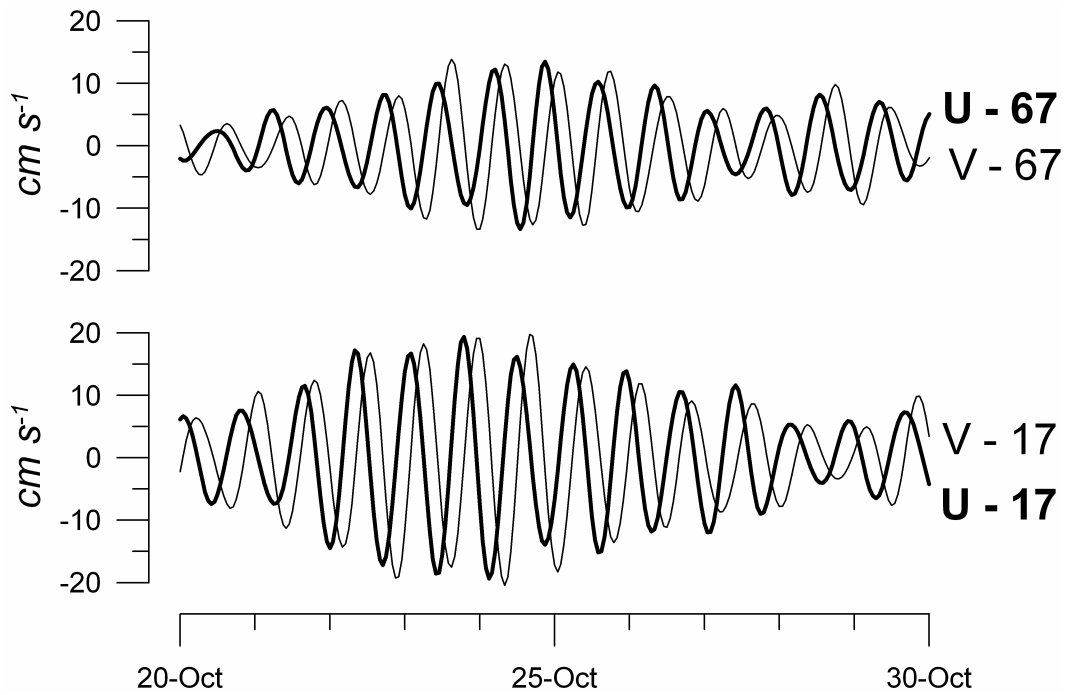
FIGURE 3 – Eastward (thick line) and northward (thin line) components of the band-pass filtered currents at 67 m and 17 m at site C. Note the almost equal magnitude of u and v, and the approximate 90° lag of v behin d u in each depth.
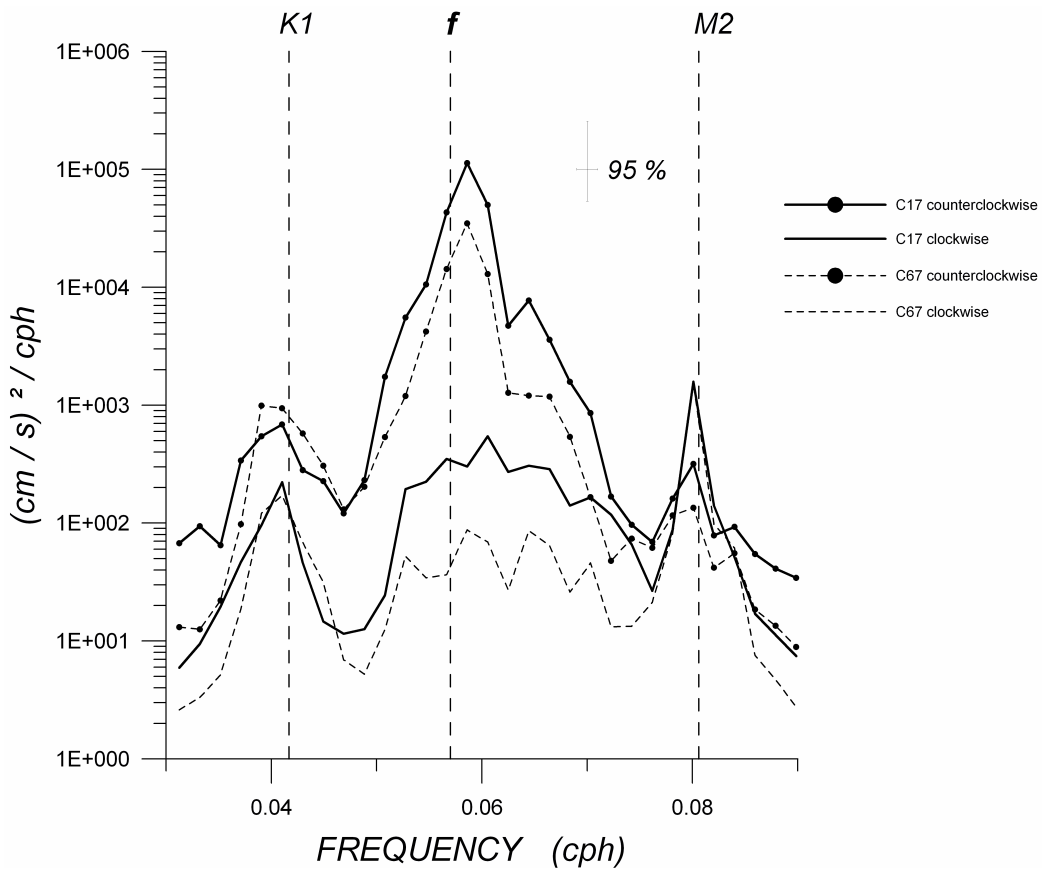

FIGURE 4 – Rotary spectra from low passed currents at site C. Near-surface currents (C17) – solid line, near-bottom currents (C67) – dotted line. Counterclockwise component – thick line, clockwise component – thin line. Vertical lines indicate the main diurnal (K$_1$) and main semi-diurnal (M$_2$) tidal frequencies and the local Coriolis frequency (f).

At both depths at site C (C17 and C67) the horizontal velocity vector describes a counterclockwise ellipse. The band-filtered series were used for computing the size and orientation of the average hodograph. The ratio between the major and minor axes is 1.04 at both depths and, according to theory (Kundu, 1976b), coincides with the ratio ω / f, where ω is the observed frequency and f is the inertial frequency. The rotary spectra (Figure 4), based on the ensemble average of pieces of 512 hourly data (frequency resolution of 0.00195 cph), confirm the frequency shift in relation to the local inertial frequency. Theory predicts that the major axis is aligned with the horizontal direction of propagation (Kundu, 1976b). Though the orientation is hard to establish with precision due to the scant eccentricity of the velocity ellipses, the orientation of the major semi-axis at both levels it is 105°T, i.e., approximately perpendicular to the coast.

During the Austral spring-summer period, there is a strong seasonal thermocline in the middle shelf area (Guerrero & Piola, 1997). Based on historical hydrographic data, Forbes & Garraffo (1988) showed that the area is characterized by a 20 to 30 m thick thermocline located at a depth of 35 to 45 m. Continuous vertical temperature-salinity (CTD) data collected in May 1992 (Charo et al., 1993) shows that the stratification at site C extends into the fall (see Figure 5). Considering the total depth of the area -approximately 97 m – the observed stratification may be represented by a two-layer model (see Millot & Crépon, 1981), with the top layer $h_1 = 40$ m and the bottom layer $h_2 = 57$ m. If the velocity at 17 m (u_1) and at 67 m (u_2) are representative of the upper and lower layer respectively, then the model predicts that $u_1 h_1 = u_2 h_2$, thus $u_1 = 1.42 u_2$. A linear regression to band-passed velocities (Figure 6.a) leads to a best fit relation of $u_1 = 1.59 u_2$ which is equivalent to $h_1 = 37$ m and $h_2 = 60$ m, fairly close to the two-layer model prediction.
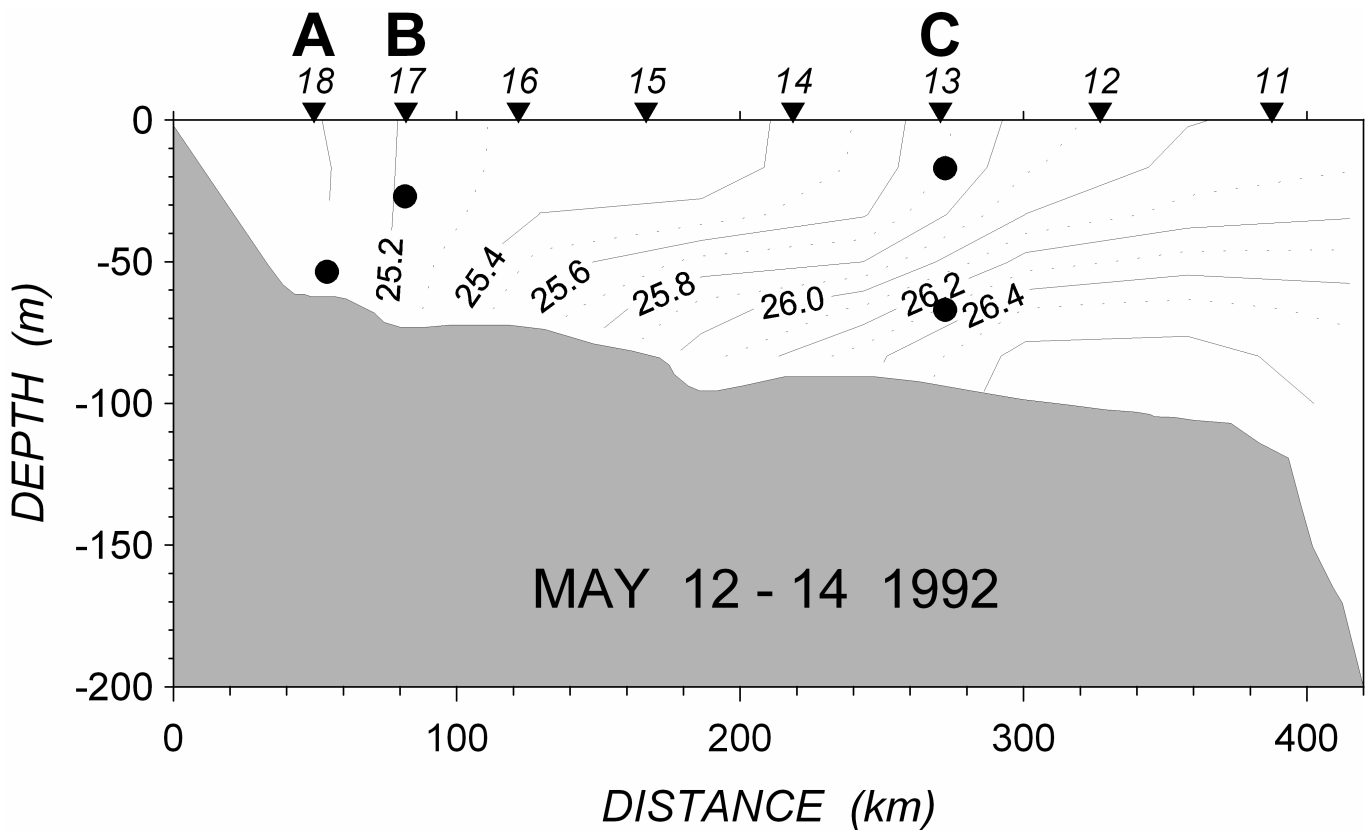

FIGURE 5 – Vertical density anomaly section (σ_T) across the continental shelf based on quasi-continuous (CTD) data collected 12 to 14 May 1992. The contour interval is 0.1 kg m^{-3} with solid lines every 0.2 kg m^{-3}. The station positions are marked along the top axis. The large dots indicate the positions of the current meters.

Figure 6.b shows the phase of the inertial signal observed at site C at 17 m versus 67 m. The dotted area illustrates the phase difference of approximately 180° found between both signals and suggests that, at least from

September to February (the period when there is data at both levels), the inertial circulation is dominated by the first baroclinic mode. Amplitudes lower than 10 cm s^{-1} produce the phase scatter away from the nearly 180° relation in Figure 6.b, suggesting a more robust phase relation at higher speeds. A quantitative estimate of the phase difference between the currents at 17m and 67m can be obtained based on the complex correlation coefficient proposed by Kundu (1976a). The method estimates the mean current veering by weighting the averaging according to the magnitude of the instantaneous current amplitudes. The complex correlation coefficient between currents at 17 m and 67 m is a complex number whose magnitude is 0.83 and whose phase angle is 176 °, which indicates a counterclockwise turn of the velocity vector as depth increases. This rotation (lower than 180 °) corresponds to a phase propagation from the bottom towards the surface, i.e., downward energy propagation, which is associated a surface generation mechanism. However, the phase estimate uncertainty (± 37°) prevents a conclusive interpretation regarding the direction of the energy propagation.
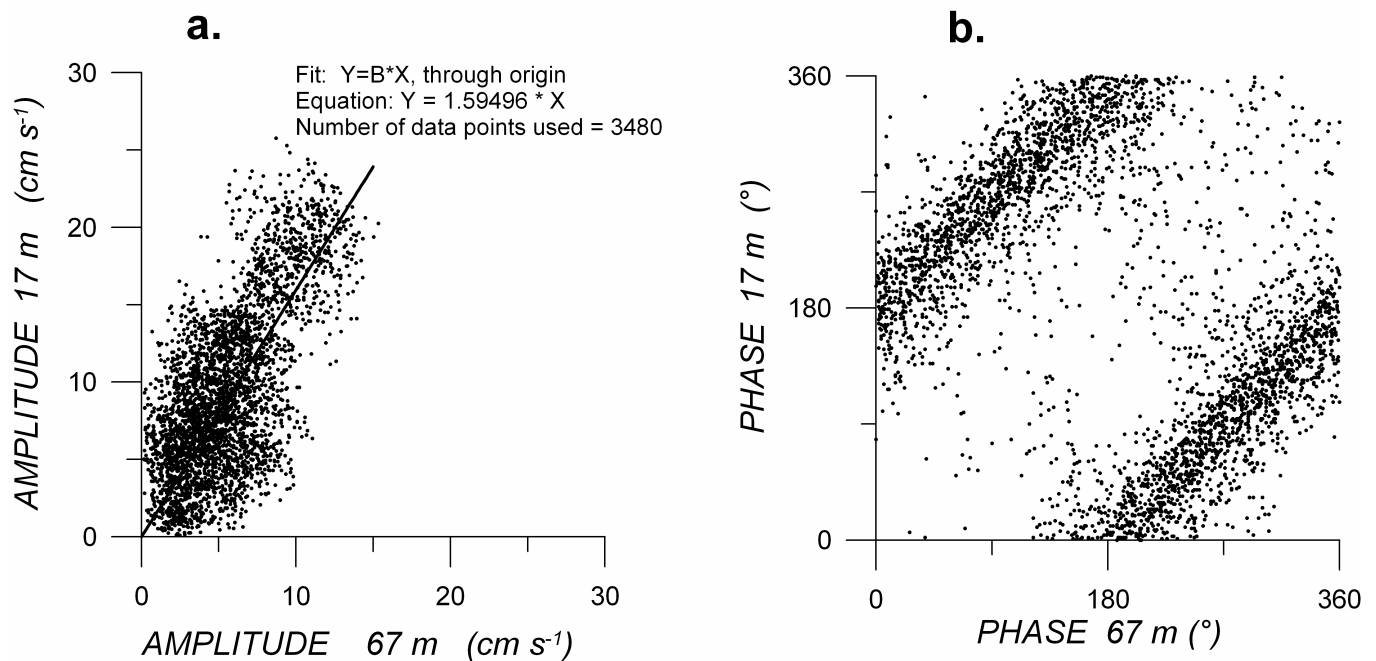

FIGURE 6 **a**. – Amplitude of band-passed observations at 17 m versus amplitude at 67 m depth at site C. The line is the best linear fit to the data. **b.** Phase of band-passed observations at 17 m versus phase at 67 m depth at site C.

3.2 – Generation of Inertial Oscillations

As mentioned above, there is general consensus in considering the wind as the main forcing generating inertial oscillations in the mixed layer. Additionally the surface intensification and the upward phase propagation found in the filtered series imply that wind stress may play the most important role in forcing the inertial oscillations. For this reason, a simple slab-like mixed layer model, driven by the observed wind stress, is introduced here to evaluate the effects of wind forcing. Pollard & Millard (1970) used a linear relation between the local wind and the current to build a simple model that simulates surface currents. The model's equation is

$$\partial_t V + \omega V = T \qquad (1)$$

where $V = u + i\,v$, $T = (\tau^x + i\,\tau^y)\,/\,\rho\,H$, $\omega = c + i\,f$, u and v are the depth-average eastward and northward velocity components, τ^x and τ^y are the eastward and northward wind stress components, H is the depth of the mixed layer, ρ is the density of the water, c is the friction coefficient and f is the local inertial frequency. The complex transport V can be written as the sum of the Ekman transport and the inertial oscillation V_I and the solution is given by:

$$V_l(t) = - \int 1/\omega \; \partial_t T \; e^{\omega(t'-t)} \; dt' \qquad (2)$$

where V_l is initialized as zero.

Based on (2) the upper layer velocity was estimated. From October to April we set a mixed layer of constant thickness H=40 m and a homogenous ocean for the rest of the year (H = 97 m) and used a friction coefficient c=1/6 days^{-1}. Using the wind data collected in Puerto Madryn, the velocity prediction for the upper layer is shown in Figure 7. Although the model predicts some of the inertial oscillation events in the sub-surface current meter (C17), not all the events are simulated (e.g. the inertial oscillations recorded in March) and some of the predicted events are not observed (e.g. the mid February situation). The model output is partly a function of parameters H and c. Adjusting these parameters does not lead to substantial changes in the simulation.
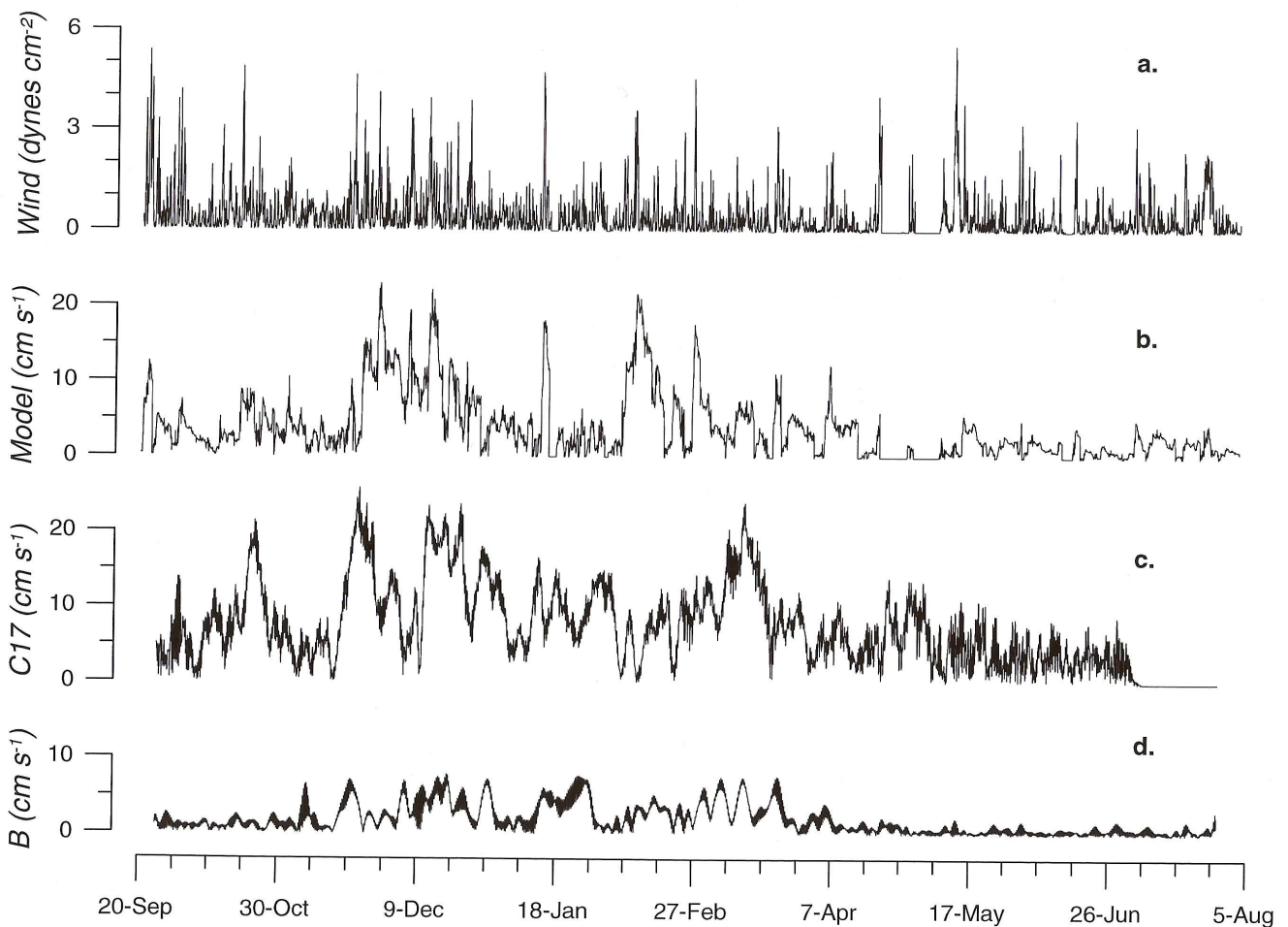

FIGURE 7 – Wind stress observed at Puerto Madryn (a), modeled amplitude of mixed layer inertial currents (b) and observed amplitude of near-surface inertial oscillations at sites C17 (c) and B (d).

The disagreement between model and observations may be due to the fact that the wind was observed more than 300 km away from site C, in an area characterized by the frequent passage of frontal systems with smaller spatial scales. Pollard (1980) pointed out that the generation of inertial oscillations is extremely sensitive to variations in the wind stress and it cannot be adequately predicted unless the local wind is known in detail. The restriction of the oscillations by a solid boundary at the coast, the effects of the variable bottom topography and the downward transfer of wind-induced energy from the upper mixed layer to the lower layer are processes not considered and can explain the poor performance of the simple linear model. In addition, Weller (1982) showed that the inclusion of the mean flow horizontal gradients in the equations of motion, produce an exponential damping of the inertial oscillations which is proportional to the horizontal divergence of the mean flow, and a frequency

displacement which is proportional to the curl of the mean flow. Because the horizontal gradients of the mean flow in this area are poorly known, we cannot evaluate this effect.

3.3 – Seasonal and Spatial Variation

Figure 2 suggests that the inertial oscillations are substantially more energetic during the Austral summer, when the water column is strongly stratified. To further analyze the 10 day to seasonal variations of the inertial oscillations, the amplitudes of the filtered currents and wind from Puerto Madryn were smoothed using a 120 element running average (Figure 8). The smoothing eliminates the fluctuations with periods shorter than 5 days. Near the coast, at sites A and B, the low-passed current velocity does not exceed 5 cm s^{-1} from November to March and is negligible (<2 cm s^{-1}) during the rest of the sampling period. In the mid-shelf mooring (site C), the inertial signal is more intense during the Austral summer (until late March), with peaks of 20 cm s^{-1}, and decays to <10 cm s^{-1} after April. The amplitude of the inertial signal at C is more intense near the surface (C17). Kundu et al. (1983) used a coastal model forced by a constant wind in order to study the coastal oscillations, and concluded that since these are circularly polarized, the condition of zero normal flow at the coast results in a quick decline there. This decline forces a downward energy flux from the surface-coast corner. The model of Kundu et al. (1983) is rigid-lid and indicates that the coastal boundary and the ocean bottom influence the flow field only near the coast. This mechanism may be useful in interpreting the observations from the coastal mooring, but does not explain the absence of oscillations in the mid-shelf mooring during the Austral winter, when the stress and the high-frequency variation of wind field is as intense as in summer (fig. 7 and 8).
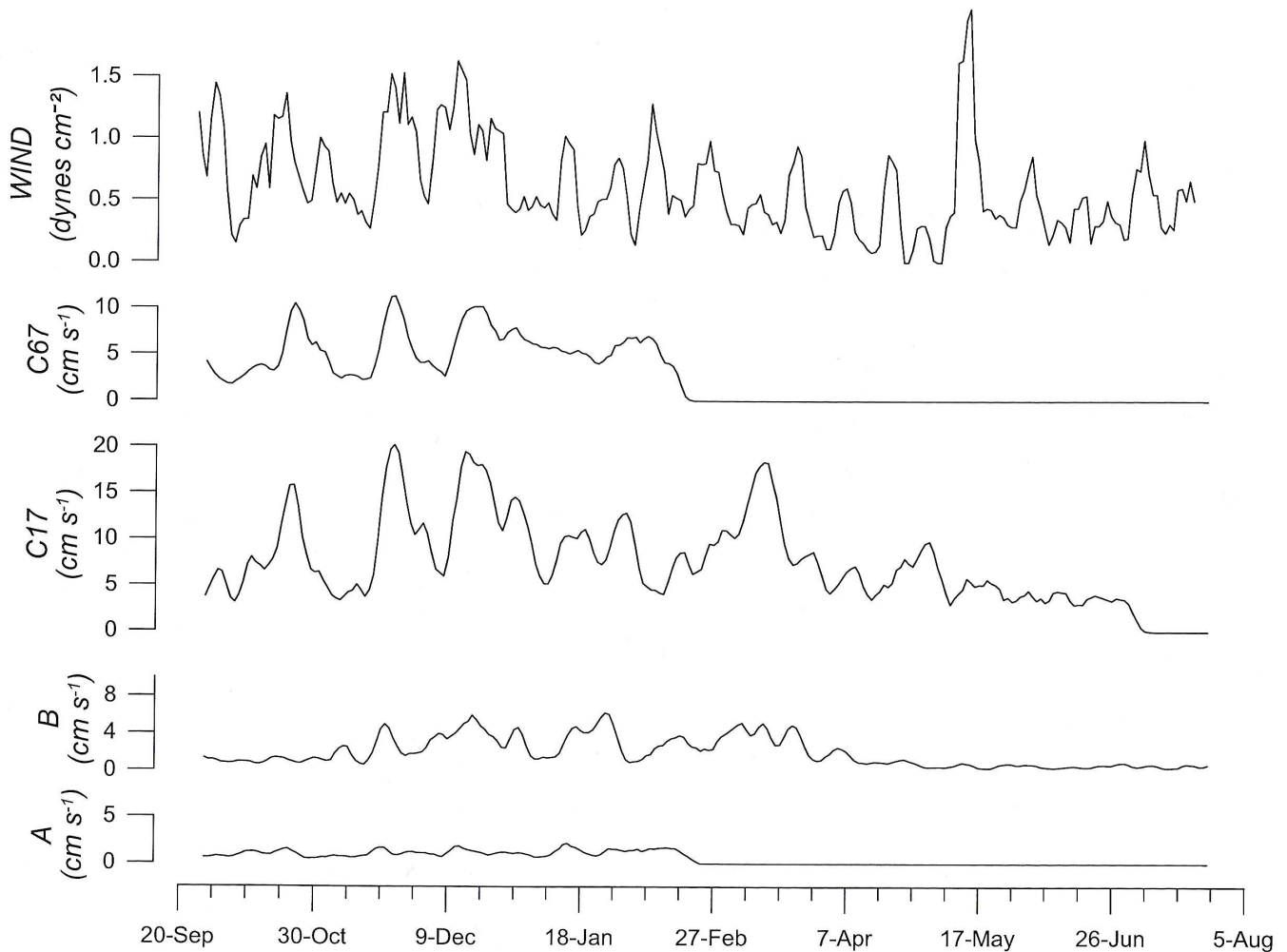

FIGURE 8 –120 hour running average of amplitudes of wind stress and inertial currents.

The seasonal variation found in the inertial oscillations is opposite to that described by D'Asaro (1985) in the Northwest Pacific. He reported that the wind energy flux towards the mixed layer is higher in the winter. Lagerloef & Muench (1987) observed that in the Bering Sea shelf the inertial oscillations are more intense during autumn and spring due to the winter decline in the cyclonic activity. Assuming that the wind recorded in Puerto Madryn is representative of the conditions over the three moorings, given that inertial oscillations are not detected at site C in Austral winter, when there is intense atmospheric activity, it is concluded that the wind is not sufficient for the generation of inertial currents in winter and that other factors are required.

Csanady (1972) analyzed the response of a stratified semi-enclosed sea to the wind stress and concluded that the first baroclinic mode dominates the inertial signal. He also showed that a stratified sea obtains much more energy from the wind than a homogeneous sea. These results suggest that not only wind but also certain stratification is required for the effective generation of inertial oscillations. In a two-layer model reproducing the damping of transverse internal seiches Krajcar & Orlic (1995) parameterized the bottom friction as proportional to the baroclinic velocity of the lower layer and the interface friction with the velocity shear and the density difference across the pycnocline. They concluded that the damping of the inertial oscillations is faster as stratification decreases. Numerical experiments with a two-dimensional coastal ocean circulation model made by Chen & Xie (1997) reproduced the cross-shelf structure of wind-induced, near-inertial oscillations observed in the Texas-Louisiana shelf. For a given spatially uniform impulse of wind (cross-shelf, along-shelf or rotating wind), when stratification is included the model predicts much stronger near-inertial oscillations than for the homogeneous case. The above results indicate that as stratification decreases the energy transfer from the atmosphere decreases and the inertial oscillations are attenuated. Historical hydrographic data reveals that in the mid-shelf region the stratification virtually reduces to zero in Austral winter while the near coastal region remains poorly stratified throughout the year. For instance, in May 1992 the Brunt-Väisälä frequency at 55 m at site C is 2×10^{-2} s^{-1} and decreases to $< 3 \times 10^{-3}$ s^{-1} in August. In contrast, at the near-shore locations the Brunt-Väisälä frequency is $< 1 \times 10^{-3}$ s^{-1} throughout the year. This explains the sharp decrease of the inertial signal in winter and suggests that the spatial distribution of inertial energy is also associated to the reduction of vertical stratification closer to shore.

Few works report significant offshore amplitude variations over realistic shelf bathymetry. Chen et al. (1996) observed inertial oscillations in spring and summer over the Texas-Louisiana shelf that have a consistent pattern in which the variance of the near-inertial currents was maximum near the ocean surface, increased in magnitude offshore to about the 200 m isobath, and then rapidly decreased further offshore. The inertial flow is characterized by a first baroclinic mode in the vertical. Chen & Xie (1997) reproduced the cross-shelf structure of these wind-induced near-inertial oscillations with a free-surface circulation model. Based on a semi-analytical theory (a simple analytical solution of the linearized horizontal momentum equations is solved using the time series calculated with the numerical model) they showed that the cross-shelf pressure gradient and the vertical gradient of Reynolds stress control the cross-shelf variation. As the model results are consistent with the analytical linear theory, they concluded that near-inertial oscillations over the continental shelf are controlled by the presence of the coast and topography. Numerical test simulations carried out by Lewis (2001) show that the cross-shelf growth of inertial amplitude does not depend on the vertical gradient of the horizontal Reynolds's stresses, the offshore transport of momentum due to internal modes, nor the non-linear advective terms in the momentum equations. He concluded that the only means by which the presence of the coastline could be felt in an offshore point is through the cross-shelf pressure gradient. A purely analytical approach (Lewis, 2001), indicates that exponentially increasing current oscillations over continental shelves are a form of inertial-gravity waves and found that the cross-shelf length-scale is significantly larger than the classical barotropic radius of deformation.

4 – SUMMARY AND CONCLUSIONS

The inertial oscillations recorded in three sites across the Argentine Continental Shelf are analyzed in detail in the present paper. It is shown that in the mooring nearest to the coast (site A) the inertial signal is barely

detectable. At site B ~49 km farther from the coast and at 27 m depth, the inertial current is observed from November to March, and the amplitude does not exceed 8 cm s^{-1}. Finally, at site C, located in the mid-shelf, the inertial signal is intense (>25 cm s^{-1}) from October to May in the sub-surface instrument (C17), and somewhat less intense (10 cm s^{-1}) in the deeper instrument (C67) from late September to February. All records show that the velocity vector is nearly circularly polarized and rotes counterclockwise with a frequency a few percent greater than the local inertial frequency. The almost 180º phase lag and the relation between the amplitudes of the inertial signal recorded by the sub-surface and the deep instrument at site C, indicate that the kinetic energy is almost exclusively contained in the first baroclinic mode. This can be interpreted as the result of a two-layer system with a solid boundary at the coast. Since the wind-induced near-inertial currents were mainly confined to the upper mixed layer, the currents in the lower layer must oscillate in an opposite phase to balance the oscillations in the upper layer and to match the boundary condition of no flux at the coast.

The simple model of Pollard & Millard (1970), forced by the wind stress, fails in reproducing the observed near-inertial oscillations. But the surface intensification and the downward energy propagation (upward phase propagation) are clear manifestations of a surface generation and imply that wind stress may be the most important forcing of such oscillations.

Csanady (1972) showed analytically that in a stratified sea the energy transfer from the wind is more efficient than in a homogeneous sea. Krajcar & Orlic (1995) with a two-layer model and Chen & Xie (1997) with a modified version of the three-dimensional coastal ocean circulation model developed originally by Blumberg & Mellor (1987), find that with stratification the near-inertial oscillations induced by the wind are much stronger than in the homogeneous case. Based on data collected from the North Sea Maas & van Haren (1987) concluded that the amplitude of the internal inertial oscillations decreases dramatically in the "unstratified" period of the year. Consequently, the theoretical analysis and the experimental results agree on the requirement of vertical stratification for the generation of inertial waves. In the vicinity of the Valdés Peninsula (43ºS) the tidal currents in the coastal area are intense enough to prevent the development of the seasonal thermocline and act to maintain the water column homogeneous throughout the year. In contrast, in the mid-shelf where the effect of the tidal turbulent steering is surpassed by the surface heat flux, a seasonal thermocline develops (Glorioso, 1987) and relatively intense inertial oscillations develop from spring to autumn. Therefore, the attenuation of the inertial currents in the coastal area and the absence of an inertial signal in the mid-shelf during the Austral winter, despite the persistence of the wind, can be explained by the reduced stratification of the water column.

Cross shelf amplitude growth in the of near-inertial oscillations to distances of order 200-300 km offshore, are not frequently observed but agree with the observations and simulations of Chen et al. (1996), Chen & Xie (1997) and Lewis (2001) in the Texas-Louisiana shelf. Lewis (2001) interprets the intensification of near-inertial energy in the offshore direction as a consequence of cross-shelf pressure gradient induced by variations of the height of the sea surface.

REFERENCES

BALESTRINI, C., A.L. RIVAS, A.R. PIOLA, A.A. BIANCHI & R.A. GUERRERO. 1996. Corrientes en la Plataforma Continental Argentina (43 ºS). Departamento Oceanografía, Servicio de Hidrogr afía Naval, Informe Técnico Nº 94, Buenos Aires, Ar gentina, 35 pp.

BLUMBERG, A.F. & G.L. MELLOR. 1987. A description of a three-dimensional coastal ocean circulation model, In HEAPS, N. S. (ed). Three-Dimensional Coastal Ocean Models, Coastal Estuarine Sci., AGU, Washington, D.C., 4: 1-6.

CHARO, M., A.P OSIROFF, A.R. PIOLA & A.A. BIANCHI. 1993. Datos físico-químicos y CTD. Campañas Oceanográficas Cap. Oca Balda 05-91, Dr. Eduardo L. Holmberg 04 y 05-92. Departamento Oceanografía, Servicio de Hidrografía Naval, Informe Técnico Nº 73, Buenos Aires, Argentina, 83 pp.

CHEN, C. & L. XIE. 1997. A numerical study of wind-induced, near-inertial oscillations over the Texas-Louisiana shelf. J. Geophys. Res., 102: 15,583-15,593.

CHEN, C., R.O. REID & W.D. NOWLIN Jr. 1996. Near-inertial oscillations over the Texas-Louisiana shelf. J. Geophys. Res., 101: 3509-3524.

CSANADY, G.T. 1972. Response of large stratified lakes to wind. J. Phys. Oceanogr., 2: 3-13.

D'ASARO, E.A. 1985. The energy flux from the wind to near-inertial motions in the surface mixed layer. J. Phys. Oceanogr., 15: 1043-1059.

FORBES, M.C. & Z.D. GARRAFFO. 1988. A note on the mean seasonal transport on the Argentinean Shelf. J. Geophys. Res., 93: 2311-2319.

GLORIOSO, P.D. 1987. Temperature distribution related to shelf-sea fronts on the Patagonian shelf. Cont. Shelf Res., 7: 27-34.

GLORIOSO, P.D. & R.A. FLATHER, 1995. A barotropic model of the currents SE South America. J. Geophys. Res, 100: 13427-13440.

GUERRERO, R.A &. A.R. PIOLA. 1997. Masas de agua en la plataforma continental. In: BOSCHI, E.E (ed.). El Mar Argentino y sus recursos pesqueros, Instituto Nacional de Investigación y Desarrollo Pesquero, Mar del Plata, 1: 107-118.

HENDERSHOTT, M.C. 1973. Inertial oscillations of tidal period. Prog. Oceanogr., 6: 1-27.

KRAJCAR, V. & M. ORLIC. 1995. Seasonal variability of inertial oscillations in the Northern Adriatic. Cont. Shelf Res., 15: 1221-1233.

KUNDU, P.K. 1976a. Ekman veering observed near the ocean bottom. J. Phys. Oceanogr., 6: 238-242.

KUNDU, P.K. 1976b. An analysis of inertial oscillations observed near Oregon coast. J. Phys. Oceanogr., 6: 879-893.

KUNDU, P.K., S.Y. CHAO & J.P. MCCREARY. 1983. Transient coastal currents and inertio-gravity waves. Deep-Sea Res., 30: 1059-1082.

KUNDU, P.K. & R.E. THOMSON. 1985. Inertial oscillations due to a moving front, J. Phys. Oceanogr., 15: 1076-1084.

LAGERLOEF, G.S.E. & R.D. MUENCH. 1987. Near-inertial current oscillations in the vicinity of the Bearing Sea marginal ice zone. J. Geophys. Res., 92: 11789-11802.

LEWIS, J.K. 2001. Cross-shelf variations of near-inertial current oscillations. Cont. Shelf Res., 21: 531-543.

MAAS, L.R.M. & J.J.M. VAN HAREN. 1987. Observations on the vertical structure of tidal and inertial currents in the central North Sea. J. Mar. Res., 45: 293-318.

MILLOT, C. & M. CRÉPON. 1981. Inertial oscillations on the continental shelf of the Gulf of Lions - Observations and theory. J. Phys. Oceanogr., 11: 639-657.

POLLARD, R.T. 1970. On the generation by winds of inertial waves in the ocean. Deep-Sea Res., 17: 795-812.

POLLARD, R.T. 1980. Properties of near-surface inertial oscillations. J. Phys. Oceanogr., 10: 385-398.

POLLARD, R.T. & R.C. MILLARD Jr. 1970. Comparison between observed and simulated wind-generated inertial oscillations. Deep Sea Res., 17: 813-821.

RIVAS, A.L., 1997. Current-meter observations in the Argentine Cont. Shelf Res., 17: 391-406.

THOMSON, R.E. & S.W. HUGGET. 1981. Wind-driven inertial oscillations of large spatial coherence. Atmosphere - Ocean, 19: 281-306.

WELLER, R.A. 1982. The relation of near-inertial motions observed in the mixed layer during JASIN (1978) experiment to the local wind stress and to quasi-geostrophic flow field. J. Phys. Oceanogr., 12: 1122-1136.